ELSEVIER

Journal of Fluids and Structures 21 (2005) 89–101

JOURNAL OF FLUIDS AND STRUCTURES

www.elsevier.com/locate/jfs

Acoustic resonance in a staggered tube array: Tube response and the effect of baffles

P.A. Feenstra[a], D.S. Weaver[a,*], F.L. Eisinger[b]

[a]*Department of Mechanical Engineering, McMaster University, Hamilton, Ont., Canada L8S 4L7*
[b]*Foster Wheeler Power Group Inc., Perryville Corporate Park, Clinton, NJ 08809-4000, USA*

Received 15 September 2004; accepted 4 June 2005

Abstract

An experimental laboratory study was performed to measure the effect of acoustic noise on the magnitude of tube vibrations in a staggered tube array and to measure the effectiveness of baffles on suppressing transverse duct modes. The acoustically induced tube vibration was experimentally determined for a flexible tube in three different transverse locations in the tube array. It was found that a tube located in the center of the duct, where a nodal point of the acoustic pressure resided, was most influenced by the transverse mode. On the other hand, a tube located near the duct side wall, where the acoustic pressure oscillation was highest, was not affected by the acoustic standing wave since it produced almost imperceptible vibration. It is shown that the acoustic pressure gradient across a tube is the cause of the tube vibration. Experiments were also performed to determine the effect of baffles for reducing the noise of acoustic resonance. The results showed that a single baffle substantially reduced the first mode resonance, as long as it was located close to the center of the bundle. The insertion of two baffles, in various locations, effectively eliminated acoustic resonance in the 1st and 2nd transverse duct modes. It is seen that the third acoustic mode is not significantly affected by either one or two baffles.

1. Introduction

Gas flows in heat exchanger tube arrays can generate a loud noise called acoustic resonance. This noise can occur when the frequency of flow periodicity generated in the array resonates with one of the transverse acoustic standing waves of the duct. The relevant standing waves are oriented in a direction normal to both the tube axis and the flow direction. When resonance occurs, an intense pure tone noise is often produced that can cause damage to the heat exchanger internals by metal fatigue and may also be harmful to plant personnel. The loudness of the noise depends upon the pressure drop across the tube array and the damping capacity of the tube bundle and duct. The most common remedy for this problem is to either avoid resonance by specifying an off-resonant flow velocity or by installing one or more anti-resonant baffles within the tube bundle to distort and suppress the resonant acoustic waves (Eisinger and Sullivan, 2003).

Reviews on the topic of vortex shedding or acoustic resonance have been published by Weaver (1993) and Blevins (1984). Most of the research on this topic has focused on identifying the periodicities of the interstitial flow or

*Corresponding author. Tel.: 905 525 9140x24907; fax: 905 572 7944.
E-mail address: weaverds@mcmaster.ca (D.S. Weaver).

0889-9746/$ - see front matter © 2005 Elsevier Ltd. All rights reserved.
doi:10.1016/j.jfluidstructs.2005.06.003

measuring the Strouhal numbers for a given tube array pattern and pitch ratio. It has been found that a given tube array can exhibit multiple Strouhal numbers and that they are highly dependent upon the pitch to diameter ratio as well as array geometry and Reynolds number (Weaver et al., 1993; Polak and Weaver, 1995). However Ziada et al. (1989a, b) showed that, for in-line array geometries, acoustic resonances may occur at Strouhal numbers which are different from those measured at off-resonant conditions. According to Blevins (1990), a predicted resonance does not occur in roughly 30–40% of the cases, either because the acoustic damping is too high or the flow rate is insufficient to initiate the resonance. Hence, there have been charts of Strouhal numbers developed from off-resonant measurements (Weaver et al., 1987; Oengören and Ziada, 1998; Ziada and Oengören, 2000), and others which are developed from acoustic resonance measurements (Chen, 1968, 1984; Fitzpatrick, 1986).

Presently, there are no reliable methods to predict acoustic damping in tube bundles and there is no generally accepted method to predict the sound pressure level of acoustic resonance (Eisinger et al., 1996). Also, there are almost no published works on the potential for oscillations of the tubes in a tube bank due to an acoustic standing wave. Blevins and Bressler (1993) developed a formula to estimate the sound pressure level of acoustic resonance. They reported measurements of Strouhal number and acoustic noise and developed a correlation to predict the loudness of the acoustic noise based upon Mach number and pressure drop across the tube array. In a recent study, Feenstra et al. (2006) showed that the test-section width affected the maximum sound pressures achieved at resonance and, in particular, that wider test-sections produced higher sound pressure levels in the first five acoustic modes than predicted by Blevins and Bressler (1993).

From the point of view of heat exchanger design, it is known that the insertion of baffles is an effective way of eliminating acoustic resonance. However, this may be costly and, in some cases, difficult because of the array geometry. Thus, it is desirable to know the minimum number of baffles and their appropriate location for maximum effectiveness. Alternatively, it may be useful to be able to predict the tube response for a given level of fluctuating acoustic pressure. Although Kacker and Hill (1974) measured the pressure on a tube in the presence of an acoustic standing wave, there appears to be no guidance in the literature for predicting tube response due to acoustic resonance in a heat exchanger. These issues of tube response and baffle effectiveness are addressed in this paper.

A large staggered tube array was studied in a wind tunnel. The tube bank falls into the category of closely spaced tube bundles that are generally, but erroneously, considered to be less prone to acoustic resonance. Three flexible tubes were instrumented with strain gauges and were positioned in three different locations of the tube array to observe the effect of a transverse acoustic noise on the magnitude of tube vibrations. A transverse acoustic standing wave was induced in the tube bank by two loudspeakers that were attached to the side wall of the test section. A microphone was inserted into the opposite wall for measuring the sound pressure levels.

Tests were also performed to examine the effect of baffles for reducing the noise of acoustic resonance and to determine the optimal location and number of baffles required. Five cases of a single baffle were tested in which the baffle divided the width of the tube bundle into the two smaller widths of varying proportions. In addition, three cases of double baffles were tested in which the baffles divided the test section into various proportions.

2. Experimental facility

The tube array used in the present study was the widest model used in the previous research by Feenstra et al. (2006). That paper presented experimental measurements for Strouhal number, sound pressure level and pressure drop for the tube array in three different test section widths and up to five acoustic modes. A plan view of the 473 tube bundle layout is shown in Fig. 1. The parameters of the bundle are, $D = 19.1$ mm, $T = 30$ mm, $L = 20.6$ mm with side spacing ratio of $T/D = 1.57$ and longitudinal spacing ratio of $L/D = 1.083$. Three of the tubes in the bundle, marked with an "x" in Fig. 1, were flexibly mounted and instrumented with strain gauges for vibration measurement. The top and bottom surfaces of the test-section were each made of 2 layers of 18 mm thick birch plywood, where the tube pattern was drilled into the inside layers using a CNC milling machine. The side walls of the test-section were made of 6 mm thick carbon steel plates for stiffness. The test-section was designed such that the cross-sectional dimensions of the duct upstream and downstream of the tube bundle were the same as those of the tube bundle and had roughly the same length as the tube bundle width. Flush-mounted static pressure taps connected to a water-filled U-tube manometer were used to measure the pressure drop across the tube bundle. This entire system was connected to the outlet of a variable speed, 50 h.p. centrifugal blower.

The wind tunnel was equipped with flow conditioning sections to produce a uniform flow velocity distribution at the test-section entrance to within 1% and a turbulence intensity of about 0.5%. Flow velocity was measured in the wind tunnel upstream of the test-section using a pitot-static probe connected to a low range pressure transducer that had an

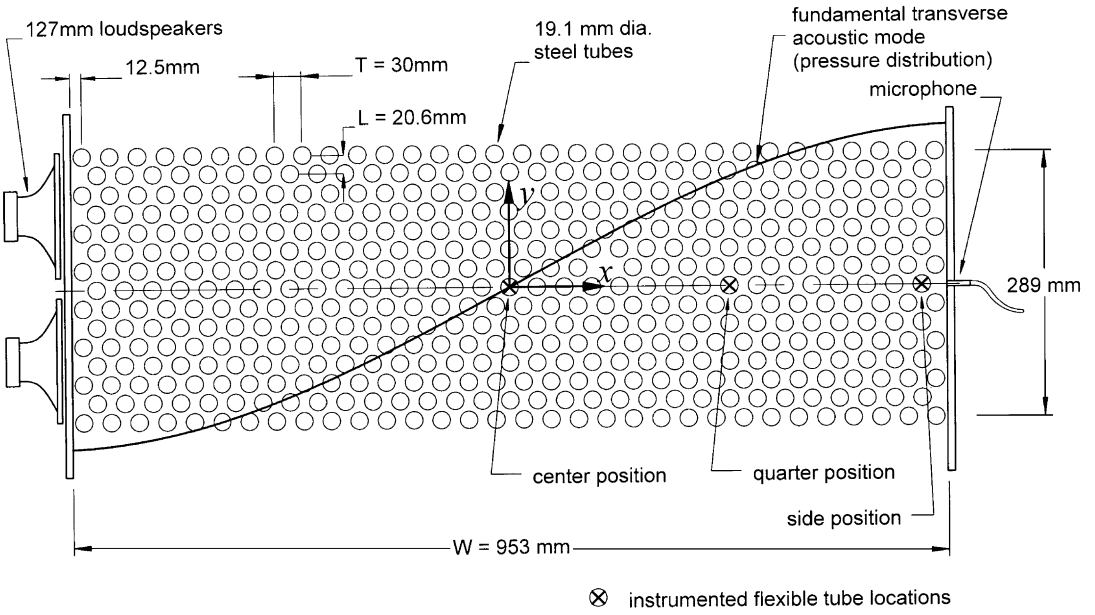

Fig. 1. Plan view of the tube bank superimposed with the fundamental transverse acoustic standing wave.

accuracy of better than $\pm 0.25\%$ of full scale. Acoustic sound pressure levels were measured using a condenser microphone with a sensitivity of 1.87 mV/Pa, a resonant frequency of 50 kHz, and an accuracy of ± 1 dB. Frequency spectra of the sound pressure measurements were obtained from an HP 35670A FFT spectral analyzer.

3. Tube response in the presence of an acoustic standing wave

Acoustic resonance is known to cause fatigue damage to the components of heat exchangers and boilers, but there is also a possibility that the tubes in the array may be excited to vibrate due to the unbalanced pressure forces on the tubes. The purpose of this part of the study was to measure the dynamic response of tubes in the presence of a transverse acoustic standing wave but in the absence of any flow through the array. As shown in Fig. 1, two loudspeakers were attached to the side of the test-section which were driven by the source output of an HP 35670A FFT analyser coupled to a two channel 150 W amplifier. A 191 Hz tone was produced at various loudness levels that closely matched the fundamental transverse acoustic mode of the duct. Measurements of tube response were obtained from a flexibly mounted and instrumented steel tube. This tube had a lowest mode natural frequency of about 180.5 Hz and a damping ratio of about 0.1% and was instrumented with strain gauges for measuring deflection in the transverse direction. The natural frequency and damping varied slightly for each experimental setup. In order to provide vibration isolation, the instrumented tube was mounted on a sturdy steel frame that was separate from the frame that supported the test-section. The instrumented tube was tested in three different locations in the array (marked with an "x" in Fig. 1) to measure the transverse response under the influence of the loudspeaker-induced transverse acoustic standing wave. During each test, rigid "dummy" tubes were mounted in the other two positions.

It was originally thought that the fluctuating acoustic particle velocity of the transverse standing wave would likely induce fluctuating forces on the tube. However, the experimental measurements indicated that the fluctuating drag coefficient required to produce the measured response varied widely and was several orders of magnitude greater than the value of 1.2 that is published in the literature for steady drag on a cylinder. Hence, it was postulated that the fluctuating acoustic pressure gradient across the tube surface was responsible for the tube vibration. The theory given below follows from this hypothesis.

A transverse force on a tube in the presence of a transverse acoustic standing wave arises from the acoustic pressure gradient across the tube. Using the coordinate system shown in Fig. 1, the spatial distribution of the acoustic pressure,

$P(x)$, in the duct width can be expressed as follows:

$$P(x) = P_0 \sin\left(\frac{\pi x}{W}\right), \tag{1}$$

where W is the test-section width and P_0 is the peak acoustic noise level. The transverse coordinate is given by x, where the origin is taken at the center of the test-section midway between the two side walls. The normal pressure distribution on the tube surface will be a function of the angle, θ, as shown in Fig. 2. To determine the pressure at any position on the tube surface, a relationship between x and θ is required as follows:

$$x = x_o + \frac{D}{2}\cos(\theta), \quad \left(x_o - \frac{D}{2}\right) \leqslant x \leqslant \left(x_o + \frac{D}{2}\right), \tag{2}$$

where x_0 is the offset distance between the center of the duct and the tube center. Using Eq. (2) in (1) gives the acoustic pressure on a tube with its center a distance x_0 from the duct centerline:

$$P(x) = P_0 \sin\left[\frac{\pi}{W}\left(x_0 + \frac{D}{2}\cos\,\theta\right)\right], \quad \left(x_o - \frac{D}{2}\right) \leqslant x \leqslant \left(x_o + \frac{D}{2}\right). \tag{3}$$

The incremental surface area of the tube (per unit of tube length) is $\mathrm{d}s = \frac{1}{2}D\,\mathrm{d}\theta$. Therefore, the acoustic pressure force on the incremental area of the tube in the direction of wave propagation (transverse direction) is

$$\mathrm{d}[w_p(x)] = P(x)\cos\,\theta\,\mathrm{d}s = \frac{D}{2}P(x)\cos\,\theta\,\mathrm{d}\theta. \tag{4}$$

The total peak force on the tube per unit length due to acoustic pressure can then be determined by integrating the force given by Eq. (4) over the circumference of the tube,

$$w_p(x_0) = 2\int_0^{\pi}\frac{D}{2}P(x)\cos\,\theta\,\mathrm{d}\theta. \tag{5}$$

Using Eq. (3) in Eq. (5) and assuming that the fluctuating drag force due to acoustic particle velocity can be included by adding, $\frac{1}{2}D\rho C_D U_{\mathrm{peak}}^2$ to Eq. (5), the total fluctuating force per unit length can be expressed as

$$w(x_0) = P_0 D\int_0^{\pi}\sin\left[\frac{\pi}{W}\left(x_0 + \frac{D}{2}\cos\,\theta\right)\right]\cos\,\theta\,\mathrm{d}\theta + \frac{D}{2}\rho C_D U_{\mathrm{peak}}^2, \tag{6}$$

where the drag coefficient of $C_D = 1.2$ is assumed, ρ is the fluid density and U_{peak} is the peak acoustic particle velocity at x_o. Eq. (6) was developed to predict the uniform peak force per unit length on the tube (at a distance x_o from the center

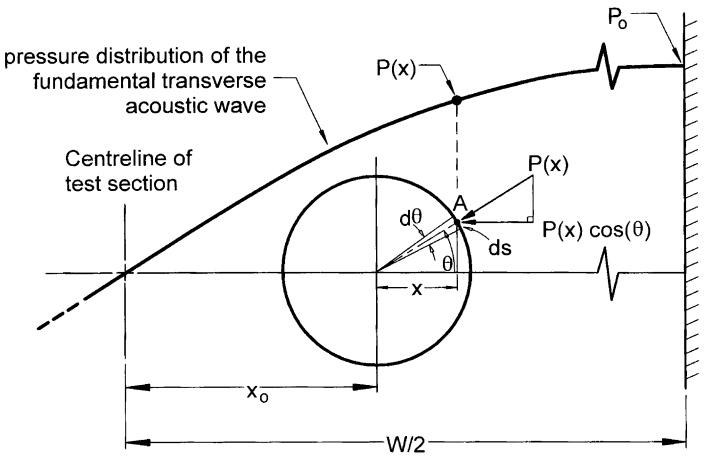

Fig. 2. Acoustic pressure distribution and instrumented tube location.

of the duct) due to the acoustic pressure field and the acoustic particle velocity of the transverse standing wave. Note that $w(x_o)$ in Eq. (6) represents a peak force per unit of tube length rather than an r.m.s. force.

In order to deduce the force per unit length on the tube from the dynamic response (strain gauge) measurements, the following vibration model was assumed:

$$y_0 = \left[\frac{w_o L^4}{8EI}\right]\left[\left(1-\left(\frac{f}{f_n}\right)^2\right)^2 + 2\zeta\left(\frac{f}{f_n}\right)^2\right]^{-0.5}, \tag{7}$$

which represents the peak tip deflection, y_0, of a uniform cantilevered beam (fixed-free) of stiffness, EI, subjected to a fully correlated transverse load over the length, L. The first term in square brackets represents the static tip deflection of the tube under uniformly distributed load, w_0, while the second term in square brackets represents the dynamic amplification factor. The latter reaches a maximum value of $(2\zeta)^{-1}$ at resonance between the applied sound frequency, f, and the tube natural frequency, f_n. Note that this model considers the fundamental vibration mode only, and higher modes are ignored. The effective peak uniform loading, w_0, can be determined by rearranging Eq. (7), since all of the other variables are known. For example, the peak tube tip amplitude, y_0, and noise excitation frequency, f, are measured in each experimental trial, while the tube length, L, tube lateral stiffness, EI, damping ratio of the tube, ζ, and the first mode natural frequency of the tube, f_n, were measured prior to the start of the experiment. Since the tube natural frequency, f_n, and the noise excitation frequency, f, were sufficiently far removed from one another, the computed results for w_0 were not significantly affected by uncertainty in the damping measurement. For simplicity in the following discussion, the force per unit length computed from the experimental measurements will be called the experimental force.

The comparison between the experimental force, w_0, (Eq. (7)) and the predicted force (Eq. (6)) for uniform tube loading is shown in Fig. 3. The data for the instrumented flexible tube mounted in the center position in the duct is shown in Fig. 3(a), while that of the same tube mounted in the quarter position is shown in Fig. 3(b). This data is also tabulated in Tables 1(a) and (b). The data for the flexible tube mounted in the side position (closest to the duct side wall) is not shown because the experimental vibration amplitudes were negligibly small and were deemed to be of little concern. The open circle symbols in Figs. 3(a) and (b) represent the experimental forces, while the open square symbols represents the predicted forces. The plus symbols represent the predicted force due to the acoustic pressure gradient alone. It is clear that the component of the force due to the acoustic particle velocity drag is very small compared to the pressure gradient component.

Comparing the experimental results in Figs. 3(a) and (b), the flexible tube mounted in the center position is subjected to higher lateral loading than when it is mounted in the quarter position. The slopes of the predicted results are linear and pass through the origin with very little scatter. Thus, the hypothesis that the acoustic pressure gradient is the cause of the tube vibration during acoustic resonance appears to be validated. However, the prediction (square symbols) underestimates the experimental results by about 25% for the center position (Fig. 3(a)) and about 19% for the quarter position (Fig. 3(b)).

One factor that may account for the difference between the experimental and predicted tube loading observed in Fig. 3 is that the local pressure distribution around the tube may not be ideal. It has been assumed that the acoustic pressure varies across the duct as a sine wave as shown in Fig. 1 and that the local pressure distribution on the tube surface is given by Eq. (3). However, it is possible that the actual local pressure distribution around the tube surface may be distorted due to the presence of the neighboring tubes. If this is the case, then the pressure distribution may be distorted in such a way that the pressure experienced by the tube is greater than predicted by the proposed model.

4. Effect of baffles on acoustic resonance

The effect of baffles on the acoustic resonance was studied for a total of five cases for a single baffle and three cases for double baffles. The noise levels measured in these tests were compared with the datum case with no baffles. The baffles used in this study were formed from 14 gauge carbon steel sheet (2 mm thick) and corrugated to fit in the tube array in a streamwise orientation. Fig. 4 shows two baffle arrangements in one illustration: a single baffle centrally located and double baffles located with roughly even spacing in the duct width. Each baffle was held securely by clamping them between the top and bottom walls of the test-section with threaded rod ties that went through the inside of a few tubes. Each end of the baffle extended about 1 tube diameter upstream and downstream of the front and back tube rows, respectively.

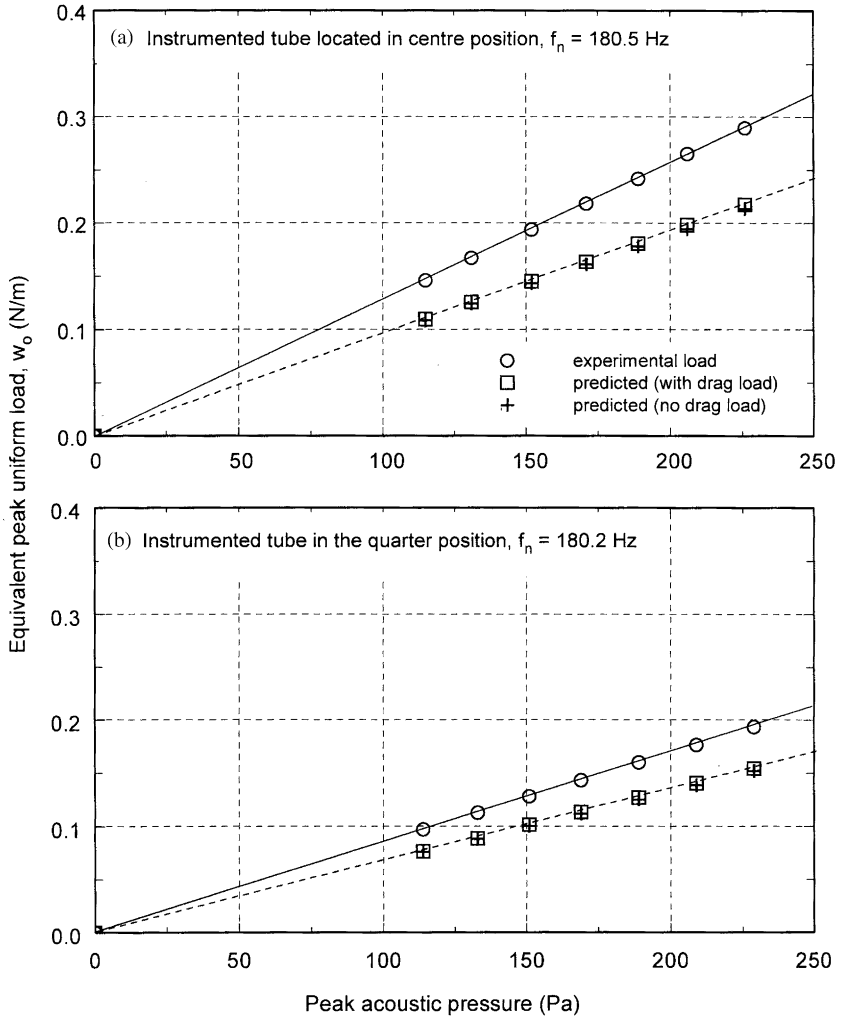

Fig. 3. Comparison between experimental and predicted acoustic loading on the flexible tube subjected to a 191 Hz transverse standing wave. Flexible tube located at the (a) center position and (b) quarter position.

Acoustic noise measurements for the datum case of no baffles is presented in Fig. 5, where the dominant frequencies of the acoustic modes and the sound pressure level amplitudes in decibels (dB) are plotted as a function of upstream flow velocity, V_u. In this figure, the dominant noise frequency for each experimental trial is indicated by a solid circle. In some trials, other peaks appeared in the frequency spectra that were also considered significant, and these secondary peaks are indicated by the open circle symbols. In most of the experimental trials, only one frequency peak was significant. The solid straight line which connects many of the frequency data points corresponds to a Strouhal number based upon average gap velocity of, $St_g = 0.41$ (or, based on upstream velocity, $St_u = 1.13$). The horizontal dashed lines correspond to the first five predicted resonance frequencies in the test-section width according to the theory of Parker (1978) for effective sound speed in a tube bundle (see, for example, Blevins, 1990).

The onset of acoustic resonance was observed in five modes corresponding to measured frequencies of approximately 188, 358, 522, 678 and 832 Hz. As shown in Table 2, the maximum noise level in each mode occurred at a slightly higher flow velocity and frequency than at the onset of the resonance. Acoustic resonance in the 1st mode occurred at an upstream flow velocity of about 3.2 m/s which corresponded to an upstream Strouhal number of $St_u = 1.14$. The noise level in this mode reached a peak amplitude of 140 dB. During this lock-in, the vibration in the top and side walls of the test-section was very perceptible to the touch. Higher mode resonances within the capacity of the wind tunnel occurred up to the fifth mode. The results of this experiment reveal that the useful range of flow velocity that avoids acoustic

Table 1
Acoustic loading on a flexible tube due to a transverse standing waves; monitored tube mounted in the center and quarter positions

Trial no.	Acoustic sound pressure level, P_{peak} (Pa)	Experimental tube tip deflection, y_{peak} (mm)	Experimental peak load on tube, w_o (N/m)	Predicted peak load on tube, w_o (N/m)
(a) Center position				
1	226	0.00386	0.290	0.218
2	206	0.00354	0.265	0.198
3	189	0.00322	0.242	0.181
4	171	0.00291	0.218	0.163
5	152	0.00259	0.194	0.145
6	131	0.00223	0.167	0.125
7	115	0.00195	0.146	0.109
(b) Quarter position				
1	229	0.00250	0.193	0.154
2	209	0.00228	0.177	0.140
3	189	0.00207	0.160	0.127
4	169	0.00185	0.143	0.113
5	151	0.00166	0.128	0.101
6	133	0.00146	0.113	0.089
7	114	0.00126	0.097	0.077

resonance is about $V_u < 3.2$ m/s, above which resonance with the first mode is encountered. There was also a narrow range of flow above this where the noise level was tolerable, between the acoustic resonances of the 1st and 2nd mode, in a flow range of about $4 < V_u < 5$ m/s.

4.1. Single baffle

Five cases of a single baffle were tested in which the baffle divided the width of the duct into two smaller widths with proportions of: 24:76, 30:70, 37:63, 43:57 and 49:51 for cases B1–B5 respectively. Fig. 6 shows the acoustic noise measurements for the case of a single baffle inserted in the test-section at roughly the middle position of the duct (case B5). In this case, the 1st mode resonance is effectively eliminated but the 2nd mode resonance at roughly 360 Hz is relatively unaffected. The resonance frequency of the 2nd mode was fairly well predicted by Parker's theory for no baffles but the higher modes showed poorer agreement. The 3rd mode resonance frequency drops from 528 Hz in the datum case to 452 Hz, and the noise level is decreased from about 165 to about 159 dB. The 4th mode is relatively unaffected while the frequency of the 5th mode is increased from about 840 to about 976 Hz. Table 3 gives the summary data for case B5 for the maximum noise level for each mode.

A comparison of the noise levels for the datum case of no baffle and the case of a single baffle are shown in Fig. 7. In this figure, the peak noise levels for each acoustic mode are presented as a function of the input energy parameter, $M\,\mathrm{d}P$, which is the Mach number in the gap flow, M, times the pressure drop, $\mathrm{d}P$, across the array. The solid line is based on the predictions of Blevins and Bressler (1993) and is discussed at some length in Feenstra et al. (2006). By comparing the noise levels for the case with no baffle (X symbol) and the single baffle cases, it is clear that the noise level of the 1st mode is reduced most significantly by a more central placement of the single baffle as in cases B3–B5. In those test cases, the 1st mode resonance is virtually eliminated. However, for the 2nd mode resonance (i.e., at roughly 360 Hz), a single baffle has little effect regardless of where it is located. The 3rd mode resonance was reduced in case B4, where a 24.2 dB drop in noise level was observed, and in case B3 where the drop was 10.5 dB. However, the general trend revealed by these tests is that a single baffle is only truly effective in suppressing the 1st mode resonance when it is located in the central region of the duct.

4.2. Double baffles

Three cases of double baffles (i.e., experiments DB1, DB2 and DB3) were also evaluated for their effect on acoustic resonance. In these cases two baffles, spaced 270 mm apart, were inserted in the array in three different positions. Fig. 8

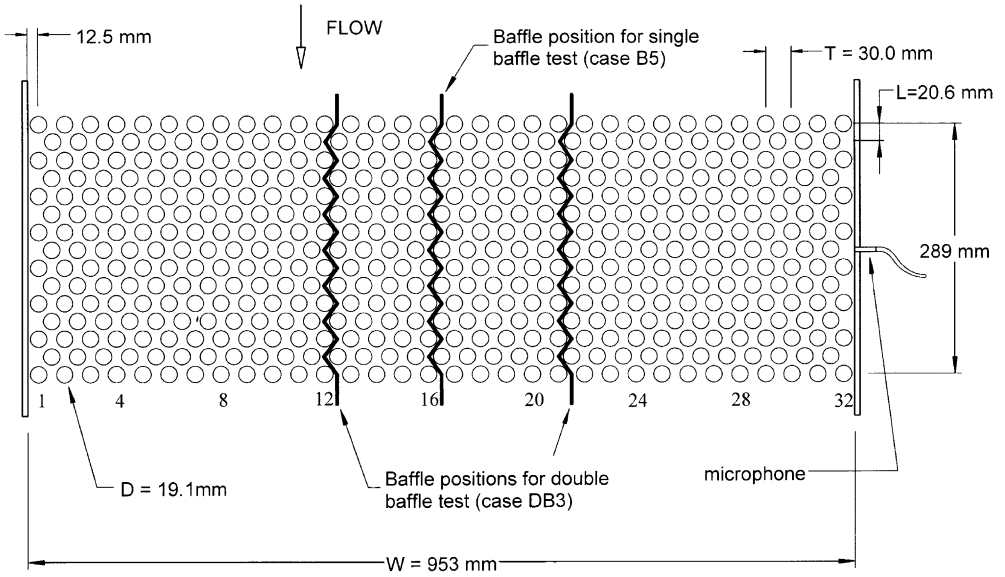

Fig. 4. Tube bundle layout and baffle locations for the single baffle case (case B5) and the double baffle case (case DB3).

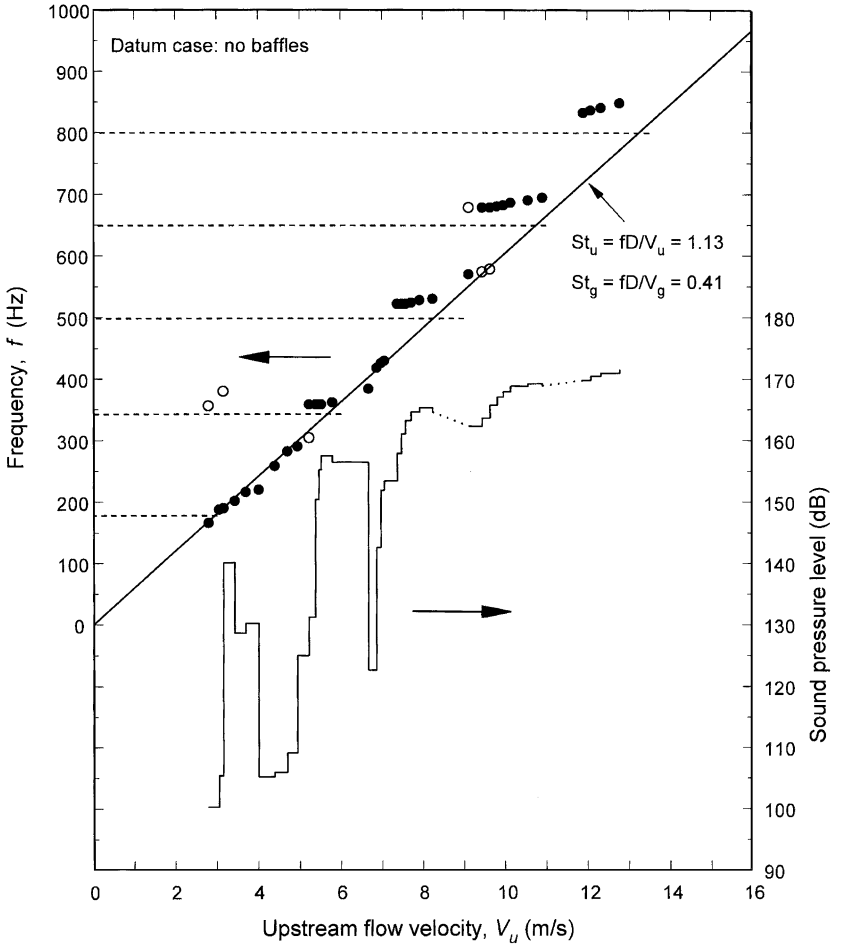

Fig. 5. Acoustic noise level and frequency measurements for the datum case of no baffles; ----, frequency prediction by Parker (1978) assuming no baffles.

Table 2
Summary of experimental results for acoustic resonance for the datum case: no baffles

Mode no.	Resonance: onset or maximum	Upstream flow velocity, V_u (m/s)	Upstream Strouhal number, St_u	Acoustic frequency, f (Hz)	$M\,dP$ (Pa)	Noise level (dB)
1	Onset	3.06	1.17	188	3.6	105.4
	Maximum	3.16	1.14	190	4.4	140.1
2	Onset	5.23	1.30	358	17.5	131.2
	Maximum	5.52	1.23	358	25.5	157.5
3	Onset	7.37	1.35	522	52.2	157.8
	Maximum	7.92	1.27	528	84.2	165.3
4	Onset	9.45	1.37	678	117.1	163.6
	Maximum	10.6	1.25	690	199.3	169.2
5	Onset	11.9	1.33	832	257.5	169.8
	Maximum[a]	12.8	1.26	848	362.1	171.5

[a]Data corresponds to the maximum flow capacity of fan.

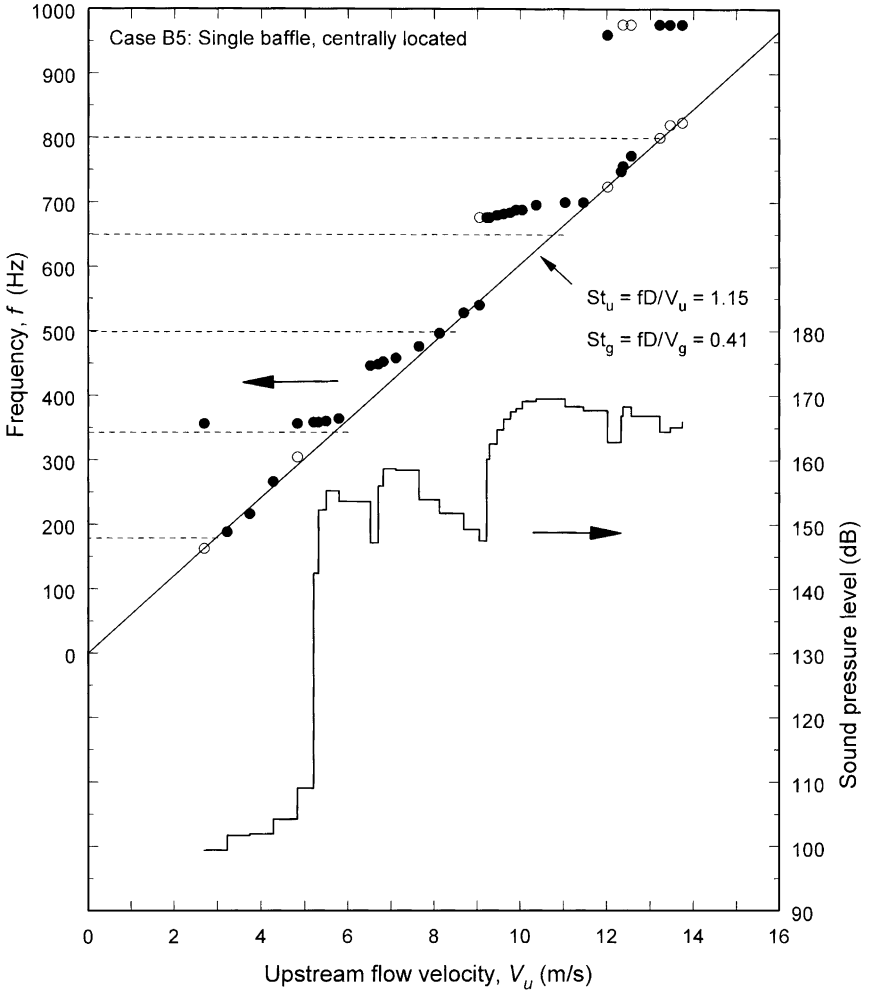

Fig. 6. Acoustic noise level and frequency measurements for the single, centrally located baffle; ----, frequency prediction by Parker (1978) assuming no baffles.

Table 3
Summary data for acoustic resonance for case B5: single baffle, centrally located in the duct

Mode no.	Upstream flow velocity, V_u (m/s)	Acoustic frequency, f (Hz)	MdP (Pa)	Noise level (dB)
1	3.22	188	4.4	101.7
2	5.50	360	24.9	155.2
3	6.82	452	48.3	158.6
4	10.4	696	189.8	169.5
5[a]	13.7	976	346	166.5

[a]Data corresponds to the maximum flow capacity of fan.

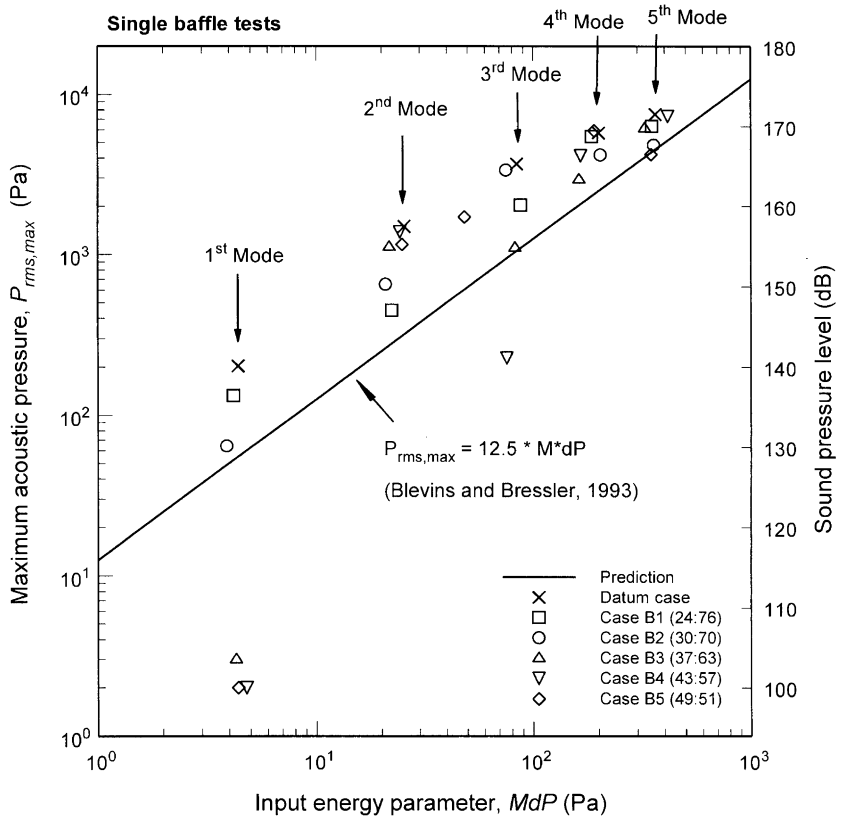

Fig. 7. Maximum acoustic pressure versus input energy parameter for the single baffle tests. Data points correspond to the maximum measured acoustic pressure for modes 1–5 (roughly). Note that the Mach number, M, corresponds to flow in the gap between tubes and that the datum case corresponds to $W = 953$ mm with no inserted baffles.

shows the noise and frequency measurements for case DB3, in which the duct width was divided into nearly even proportions (i.e., 37:28:35). In this case, it is clear that resonances in the 1st and 2nd modes were effectively eliminated. This was observed for all the test cases, indicating that precisely even spacing of the two baffles is not necessary in order to eliminate acoustic resonance in the 1st and 2nd modes. The frequency prediction of Parker (1978) assuming no baffles was fairly good for the 3rd mode but poorer for the higher modes. Table 4 gives the summary data for case DB3 for the maximum noise levels for each mode.

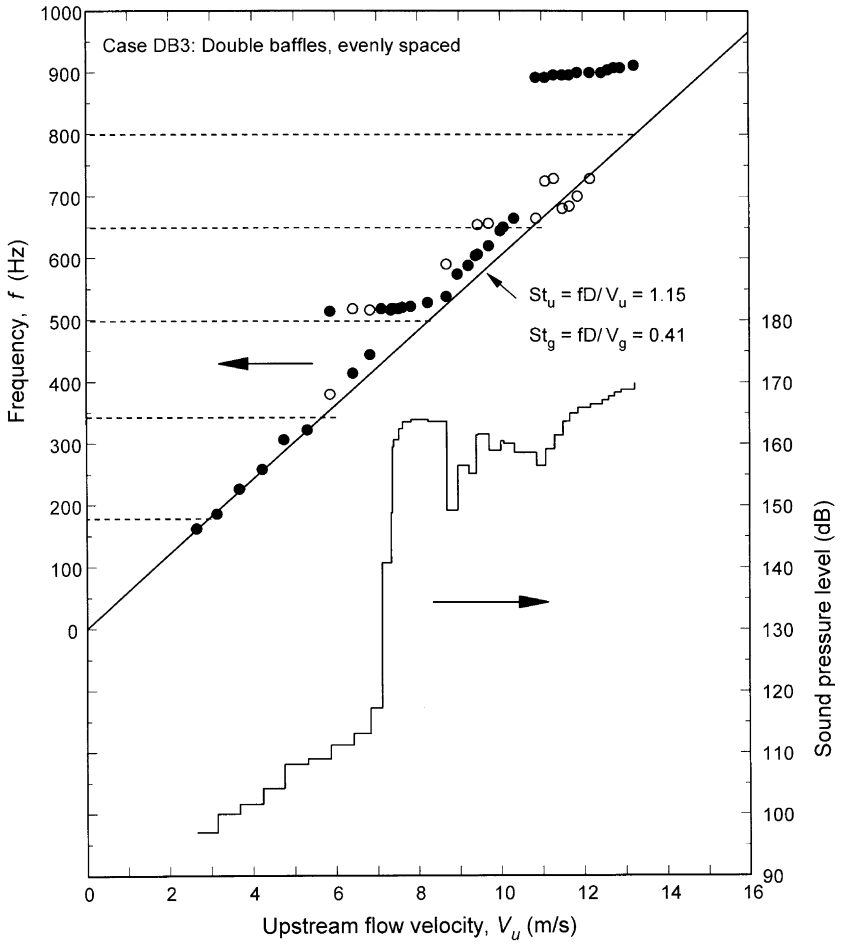

Fig. 8. Acoustic noise level and frequency measurements for case DB3 for a double baffle (spaced 37:28:35); ----, frequency prediction by Parker (1978) assuming no baffles.

Table 4
Summary data for acoustic resonance for case DB3: double baffles, evenly spaced in the duct

Mode no.	Upstream flow velocity, V_u (m/s)	Acoustic frequency, f (Hz)	MdP (Pa)	Noise level (dB)
1	3.15	186	4.3	100.0
2	5.32	322	19.9	109.0
3	7.83	522	75.5	163.9
4	10.3	664	158.5	158.5
5[a]	13.2	912	340.6	169.8

[a]Data corresponds to the maximum flow capacity of fan.

A summary of the results for a double baffle cases is shown in Fig. 9, where a comparison between the noise levels for the datum case of no baffle and the case of the double baffles is shown. In this case, it is clear that all of the double baffle cases essentially eliminated resonances in the 1st and 2nd modes. For the higher acoustic modes, the effectiveness of the double baffles was substantially less, with resonance noise levels exceeding 155 dB regardless of the baffle location.

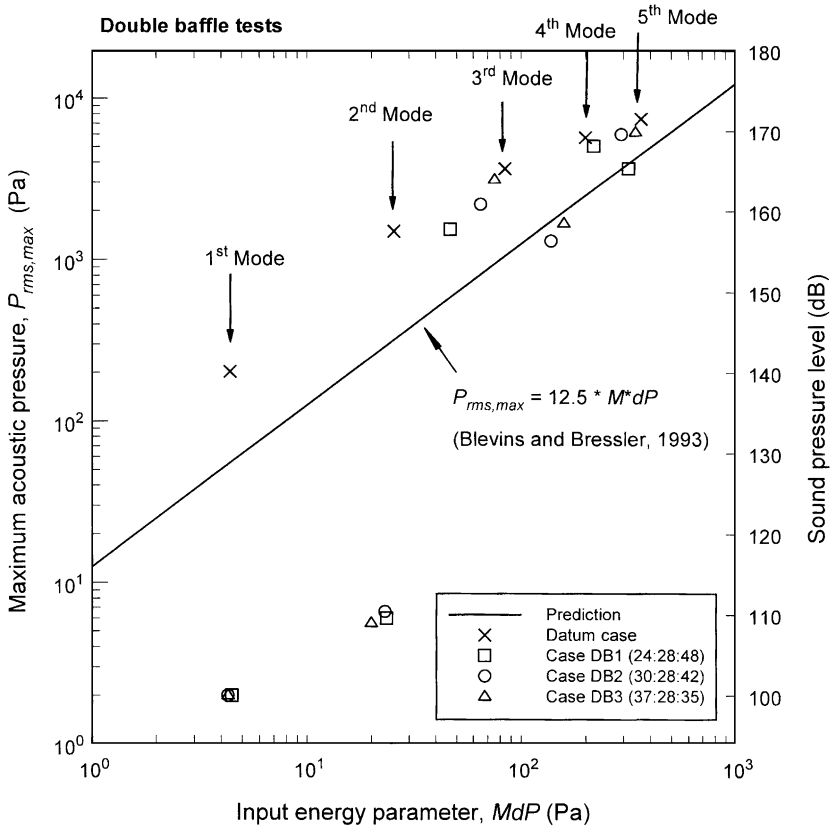

Fig. 9. Maximum acoustic pressure versus input energy parameter for the double baffle tests. Data points correspond to the maximum measured acoustic pressure for modes 1–5 (roughly). Note that the Mach number, M, corresponds to flow in the gap between tubes and that the datum case corresponds to $W = 953$ mm with no inserted baffles.

5. Conclusions

A study was carried out on acoustic resonance in a staggered tube array. The effects of acoustic standing waves on tube response and of the effectiveness of baffles in suppressing acoustic resonance were examined. The general conclusions drawn from this research are as follows.

(i) Tubes in an array can be excited to vibrate when subjected to an acoustic standing wave within the duct. The source of the excitation is apparently the pressure gradient across the tube due to the acoustic standing wave. The highest tube loading occurred when the tube was located at an acoustic pressure node (i.e., pressure was lowest) but this is also where the pressure gradient across the tube is highest. For a fundamental transverse duct mode, the maximum tube vibration occurred when the tube was located in the center of the duct. The simple theory presented in this paper under-predicted the magnitude of the acoustic tube loading, but the trend with peak noise level was correctly predicted.

(ii) The insertion of a single baffle plate in the test-section effectively eliminated the 1st mode resonance as long as the baffle was located near the center of the duct. For the 2nd and higher acoustic modes, some noise reduction was achieved. However, from a design standpoint, these experiments showed that a single baffle cannot be relied upon to suppress any but the 1st mode.

(iii) The insertion of double baffles effectively eliminated the 1st and 2nd mode resonances for all three cases tested. Precise spacing of the baffles in the duct width was not necessary to achieve this effect. Two baffles had some effect on the 3rd mode resonance but, in general, were not effective in eliminating the 3rd and higher mode resonances.

Acknowledgments

The authors are grateful to Foster Wheeler Power Group, Inc. for sponsoring this research and for their permission to publish the results.

References

Blevins, R.D., 1984. Review of sound induced by vortex shedding from cylinders. Journal of Sound and Vibration 92, 455–470.

Blevins, R.D., 1990. Flow-Induced Vibration, second ed. Van Nostrand Reinhold, New York.

Blevins, R.D., Bressler, M.M., 1993. Experiments on acoustic resonance in heat exchanger tube bundles. Journal of Sound and Vibration 164 (3), 503–533.

Chen, Y.N., 1968. Flow-induced vibration and noise in tube banks of heat exchangers due to Von Karman streets. ASME Journal of Engineering for Industry 90, 134–146.

Chen, Y.N., 1984. Flow-induced vibrations of in-line heat exchangers. In: Paidoussis, M.P., Chenoweth, J.M., Bernstein, M.D. (Eds.), Proceedings of ASME Symposium on Flow Induced Vibrations, vol. III, Vibration in Heat Exchangers. ASME, New York, pp. 163–170.

Eisinger, F.L., Sullivan, R.E., 2003. Suppression of acoustic waves in steam generator and heat exchanger tube banks. ASME Journal of Pressure Vessel Technology 125, 221–227.

Eisinger, F.L., Francis, J.T., Sullivan, R.E., 1996. Prediction of acoustic vibration in steam generator and heat exchanger tube banks. ASME Journal of Pressure Vessel Technology 118, 221–236.

Feenstra, P.A., Weaver, D.S., Eisinger, F.L., 2006. The effect of test section width on acoustic resonance in a staggered tube array. ASME Journal of Pressure Vessel Technology, submitted for publication.

Fitzpatrick, J.A., 1986. A design guide proposal for avoidance of acoustic resonances in in-line heat exchangers. ASME Journal of Vibrations, Acoustics, Stress, and Reliability in Design 108, 296–300.

Kacker, S.C., Hill, R.S., 1974. Flow over a circular cylinder in the presence of standing sound waves. Report No. Tb. 30A. Department of Mechanical Engineering, University of Newcastle Upon, Tyne, UK.

Oengören, A., Ziada, S., 1998. An in-depth study of vortex shedding, acoustic resonance and turbulent forces in normal triangular tube arrays. Journal of Fluids and Structures 12, 717–758.

Parker, R., 1978. Acoustic resonances in passages containing banks of heat exchanger tubes. Journal of Sound and Vibration 57, 245–260.

Polak, D.R., Weaver, D.S., 1995. Vortex shedding in normal triangular tube arrays. Journal of Fluids and Structures 9, 1–17.

Weaver, D.S., 1993. Vortex shedding and acoustic resonance in heat exchanger tube arrays. In: Au Yang, M.K. (Ed.), Technology for the 90's. ASME, New York, pp. 778–810.

Weaver, D.S., Fitzpatrick, J.A., ElKashlan, M., 1987. Strouhal numbers for heat exchanger tube arrays in cross-flow. ASME Journal of Pressure Vessel Technology 109, 219–223.

Weaver, D.S., Lian, H.Y., Huang, X.Y., 1993. Vortex shedding in rotated square tube arrays. Journal of Fluids and Structures 7, 107–121.

Ziada, S., Oengören, A., 2000. Flow periodicity and acoustic resonance in parallel triangular tube bundles. Journal of Fluids and Structures 14, 197–219.

Ziada, S., Oengören, A., Buhlmann, E.T., 1989a. On acoustical resonance in tube arrays, Part I: Experiments. Journal of Fluids and Structures 3, 293–314.

Ziada, S., Oengören, A., Buhlmann, E.T., 1989b. On acoustical resonance in tube arrays, Part II: Damping criteria. Journal of Fluids and Structures 3, 315–324.